6. Voûete PA, Hoefnagel CA, De Kraker J. Iodine-131-meta-iodobenzylguanidine in diagnosis and treatment of neuroblastoma. *Cancer* 1988;75:107–111.
7. Bomanji J, Conry BG, Britton KE, Reznek RH. Imaging neural crest tumors with ^{123}I-metaiodobenzylguanidine and x-ray computed tomography. A comparative study. *Clin Radiology* 1988;39:502–506.
8. Müller-Gärtner HA, Ertmann R, Helmke K. Meta-iodobenzylguanidine scintigraphy in neuroblastoma. A comparison with conventional x-ray and ultrasound. *Pediatr Hematol Oncol* 1986;3:37–47.
9. Lastoria S, Maurea S, Caraco C, et al. Iodine-131-metaiodobenzylguanidine scintigraphy for localization of lesions in children with neuroblastoma: comparison with computed tomography and ultrasonography. *Eur J Nucl Med* 1993;20:1161–1167.
10. Lebtahi-HadjDjilani N, Lebtahi NE, Bischof-Delaloye A, Laurini R, Beck D. Diagnosis and follow-up of neuroblastoma by means of iodine-123-metaiodobenzylguanidine and bone scan, and the influence of histology. *Eur J Nucl Med* 1995;22:322–329.
11. Vogler JB, Murphy WA. Bone marrow imaging. *Radiology* 1988;168:679–693.
12. Cohen MD, Klatte EC, Baehner R, et al. Magnetic resonance imaging in children. *Radiology* 1984;151:715–718.
13. Tanabe M, Takahashi H, Ohnuma N, Iwai J, Yoshida H. Evaluation of bone marrow metastasis of neuroblastoma and changes after chemotherapy. *Med Pediatr Oncol* 1993;21:54–59.
14. Corbett Rolliff J, Fairley N, Moyes J, et al. A prospective comparison between magnetic resonance imaging, meta-iodobenzylguanidine scintigraphy and marrow histology/cytology in neuroblastoma. *Eur J Cancer* 1991;27:1560–1564.
15. Benz-Bohm G, Gross-Fengels W, Wiedemann B, Linden A. Knochenmarkmetastasierung bei Neuroblastom. MRT im Vergleich zur Knochenmarkzytologie und MIBG-Szintigraphie. *Fortschr Röntgenstr* 1990;152:523–527.
16. Bourliere-Najean B, Siles S, Panuel M, et al. Value of MRI and ^{123}I-MIBG sintigraphy in the diagnosis of spinal bone marrow involvement in neuroblastoma in children. *Pediatr Radiology* 1992;22:443–446.
17. Couanet D, Geoffray A. Etude en imagerie par résonance magnétique (IRM) des métastases ostéomédullaires de neuroblastomes. *Bull Cancer* 1988;75:91–96.
18. Weinreb JC. MR Imaging of bone marrow: a map could help. *Radiology* 1990;177:23–24.
19. Ricci C, Cova M, Kang YS, et al. Normal age related patterns of cellular and fatty bone marrow distribution in the axial skeleton: MR imaging study. *Radiology* 1990;177:83–88.

Manipulation of Blood Clearance to Optimize Delivery of Residualizing Label-Antibody Conjugates to Tumor Cells In Vivo

Rhona Stein, David M. Goldenberg, Gaik Lin Ong, Suzanne R. Thorpe and M. Jules Mattes

Garden State Cancer Center, Center for Molecular Medicine and Immunology, 520 Belleville Avenue, Belleville, New Jersey; and Department of Chemistry and Biochemistry, University of South Carolina, Columbia, South Carolina

We have attempted to improve the therapeutic index of radioimmunotherapy by manipulating the blood clearance rate and the catabolism of the radiolabel. The general strategy is to allow the antibody (Ab) to circulate in the blood for 2–3 days, then to clear it rapidly by a method that delivers the Ab to hepatocytes. In addition, the radiolabel selected has two key properties: it is a residualizing label (which is lysosomally trapped after catabolism), so it is retained well by tumor cells, but is excreted rapidly by hepatocytes into bile. **Methods:** In initial experiments, three residualizing radiolabels were tested for their rate of excretion after specific delivery in vivo to either hepatocytes, via galactosylated Ab, or Kupffer cells, via immune complexes. A label showing rapid biliary excretion only after delivery to hepatocytes, ^{111}In-benzyl-diethylenetriamine tetraacetic acid, was then used for radioimmunodetection in a protocol of delayed rapid blood clearance in which clearance was by hepatocytes. This was achieved by using galactosylated Ab, combined with temporary inhibition of the asialo-glycoprotein receptor on hepatocytes. Ab RS11 and the lung adenocarcinoma Calu-3 xenograft in nude mice were used. Control experiments were performed with a conventional ^{125}I label and with ^{125}I-dilactitol-tyramine. **Results:** Indium-benzyl-diethylenetriamine tetraacetic acid was identified as a label that was excreted more rapidly from hepatocytes than from Kupffer cells, by biliary excretion. Using this radiolabel with delayed rapid blood clearance, very high tumor/blood ratios were obtained, 166:1 at day 3, but tumor/normal tissue ratios for other tissues were not as high. There appeared to be some uptake of the radiolabel by all normal tissues tested, including the lungs and muscle. Dosimetry calculations suggested that the therapeutic index was no better than with a simple Ab injection. **Conclusion:** Antibody catabolism can be directed towards either hepatocytes or Kupffer cells, and this difference can strongly affect the excretion rate of radiolabels, since only hepatocytes can excrete degradation products into bile. Processing will also depend on the particular radiolabel. These factors are particularly important for protocols involving delayed rapid blood clearance, since liver uptake is so rapid. The methods described should stimulate other approaches of manipulating Ab blood clearance and radiolabel catabolism to achieve improved therapeutic results.

Key Words: antibody localization to tumors; residualizing radiolabels; rapid blood clearance of antibodies; antibody catabolism in liver

J Nucl Med 1997; 38:1392–1400

Use of antibody (Ab)–radioisotope conjugates to specifically deliver radiation to tumors has been the focus of many experimental studies, with some recent encouraging clinical results (*1*). The most widely used strategy is the simplest approach; namely, injecting radiolabeled Abs. However, there are many possible methods of modifying this basic approach with the aim of increasing the therapeutic index. For the reasons described below, we have combined three modifications: (a) induction of delayed rapid blood clearance of the Ab after 2–3 days of circulation (slow clearance followed by rapid clearance), (b) use of a residualizing radiolabel (a label which is trapped within the cell after catabolism of the Ab to which it was originally conjugated) and (c) clearance by hepatocytes rather than macrophages and Kupffer cells.

Rationale for Delayed Rapid Blood Clearance

The major toxicity resulting from radioimmunotherapy is myelotoxicity, resulting primarily from the radiation dose delivered by circulating Ab to the bone marrow. Because Abs bind specifically at the tumor site, and because blood clearance of immunoglobulin G (IgG) is quite slow, it seems useful to induce rapid blood clearance after the tumor has been maximally penetrated by the Ab, which may be expected to take 2–3 days (*2,3*). This would be particularly advantageous if saturating levels of Ab have been used, since no further binding to the tumor cells can occur. Delayed rapid blood clearance has been

Received Jul. 8, 1996; accepted Dec. 10, 1996.

For correspondence or reprints contact: M. Jules Mattes, Center for Molecular Medicine and Immunology, 520 Belleville Avenue, Belleville, NJ 07103.

achieved by several approaches. The most widely used method has been a two-step protocol that involves complexation of the Ab with some type of cross-linking agent, which can be a second Ab or avidin (if biotinylated Abs are used) (*4–7*). A second approach is to use galactosylated Abs (gal-Abs) in combination with asialo-bovine submaxillary mucin (asialo-BSM) (*8*). In this case, the gal-Ab would normally be rapidly cleared from the blood by the hepatic asialoglycoprotein (ASGP) receptor, but this uptake can be blocked temporarily by the injection of competitive inhibitors that bind to the ASGP receptor, such as asialo-BSM. A third approach is extracorporeal immunoadsorption (*9*), which is the simplest in theory and avoids many of the problems discussed below, but is cumbersome in practice.

Rationale for Use of a Residualizing Radiolabel

It has been found that when a two-phase clearance system is used, Ab localized at the tumor site also decreases substantially after the Ab is cleared from the blood (*4,5,7–9*). This factor limits the effectiveness of this approach. Such loss of bound Ab can be attributed to three factors: (a) removal of unbound, circulating Ab from the blood and interstitial fluid within the tumor; (b) dissociation of bound Ab; and (c) internalization and catabolism of bound Ab, with release from the cell of catabolic products. This third factor can be circumvented by the use of "residualizing" radiolabels (*10,11*). We have recently described a nude mouse xenograft model system, Ab RS11 localizing to the human lung carcinoma Calu-3, in which the use of residualizing radiolabels (without a two-phase clearance) provided a large advantage for radioimmunotherapy (*11*). Thus, it seems logical to combine the use of a residualizing label with two-phase clearance.

Rationale for Use of a Clearance Mechanism that Selectively Delivers Abs to Hepatocytes

A factor that limits the value of residualizing labels is that these labels are also retained in any cells that take up the Ab by normal metabolic processes. Thus, we demonstrated that the liver, spleen and kidney have some tendency to accumulate residualizing labels (*11*). This factor would be expected to become especially prominent if a rapid clearance mechanism is used, since Ab cleared from the blood must be distributed elsewhere. In fact, all of the mechanisms used for rapid blood clearance (except for extracorporeal immunoadsorption) deliver the Ab efficiently and selectively to the liver and, in some cases, the spleen. In an effort to reduce the magnitude of this effect, we took the following approach. Among cells in vivo, hepatocytes have one unique property; namely, being capable of directly delivering catabolic products into the bile. Indeed, it has been suggested that undigestible material within lysosomes of hepatocytes is eliminated into bile by exocytosis (*12,13*). Of the methods used for rapid blood clearance, only one, the use of gal-Abs and inhibitors of the ASGP receptor, delivers the Ab selectively to the hepatocytes. In contrast, complexation methods would tend to deliver the labeled Ab to Kupffer cells (*14,15*) (some "hybrid" methods are described in the Discussion). Accordingly, initial experiments were set up to select a label that is excreted more efficiently by hepatocytes than by Kupffer cells. Previous investigations by Arano et al. demonstrated that certain labels are in fact catabolized and excreted more rapidly by hepatocytes than by Kupffer cells (*16,17*). A major purpose of this study was to test the radiolabels available to us in this respect, and a major conclusion is that ^{111}In-benzyl-diethylenetriamine tetraacetic acid (benzyl-DTPA) does in fact have the desired property.

MATERIALS AND METHODS

Antibodies and Cell Lines

Mouse monoclonal antibodies RS11, MA103 and TA99 were described previously (*2,11*). RS11 reacts with the integral cell surface glycoprotein EGP-2 (*18*). Chimeric LL2 is a human/mouse hybrid Ab that has been described (*19*), and hLL2 is a humanized mouse monoclonal antibody that retains only the hypervariable regions of the original mouse Ab (*20*). Rabbit anti-human IgG (no. 55008) was purchased from Cappell Laboratories (Cochranville, PA). Calu-3 is a human nonsmall cell long carcinoma cell line and was cultured as described (*11*).

Radiolabeling, Galactose Conjugation and Formation of Immune Complexes

Either sodium ^{125}I or ^{131}I was used, as indicated in the text. Methods have been described for labeling Ab with iodine by a conventional chloramine-T procedure (*8*), with I-dilactitol tyramine (DLT) (*11*), with I-5-([4,6-dichlorotriazin-2-yl]amino)fluorescein (DTAF) (*21*) and with ^{111}In-isothiocyanate-benzyl-DTPA (*11*). The method for galactose conjugation was also described previously (*8*). To form immune complexes, the radiolabeled humanized Ab (either chimeric or fully humanized) was incubated with a 100-fold molar excess of rabbit anti-human IgG and incubated 1 hr at room temperature before injection into mice. Complexes were analyzed by gel filtration HPLC, and >90% of the counts per minute (cpm) were in large complexes.

Biodistribution Experiments in Normal Mice

CF1 outbred female mice, 2–5 mo of age, were intravenously injected with 10^6 cpm in 0.3 ml into the suborbital plexus of the eye. The galactosylated Ab used was either TA99 or MA103, both IgG_{2a}s, which were used interchangeably and produced identical results. At various times mice were bled into preweighed tubes and killed. The entire liver, spleen, small intestine, large intestine and one kidney were collected. The intestines were collected together with their contents. Kidney data were multiplied by two to obtain cpm per organ. The total blood weight was assumed to be 7.4% of the total mouse weight. In preliminary experiments, the time of peak liver uptake was determined, and this was used for the first time point. This was 5 min for galactose conjugates and 15 min for immune complexes. In some experiments, mice were housed in metabolism cages lined with absorbent paper and the dried feces collected and counted.

Radioimmunodetection Experiments in Tumor-Bearing Nude Mice

Female outbred nude mice were injected subcutaneously with 2×10^7 Calu-3 cells, as described (*11*). When tumors were approximately 0.3–0.5 cm in diameter, the mice were injected intraperitoneally with radiolabeled galactosylated RS11, together with 25 mg asialo-BSM. Asialo-BSM was prepared by desialylating BSM as described (*8*). The mice were injected with 2–3 additional doses of 25 mg asialo-BSM, at intervals of 8–12 hr, to block the ASGP receptor for 2–3 days, as described (*8*). At various times, mice were bled and killed, and organs were collected and counted for radioactivity. Dosimetry was calculated as described (*11*).

RESULTS

Identification of a Residualizing Radiolabel Catabolized and Excreted more Rapidly by Hepatocytes than by Kupffer Cells

There were two reasons for identifying a label with this property. First, of the methods that have been used to induce rapid blood clearance of Abs, some deliver the Ab to hepatocytes and others to Kupffer cells and macrophages. Thus, the

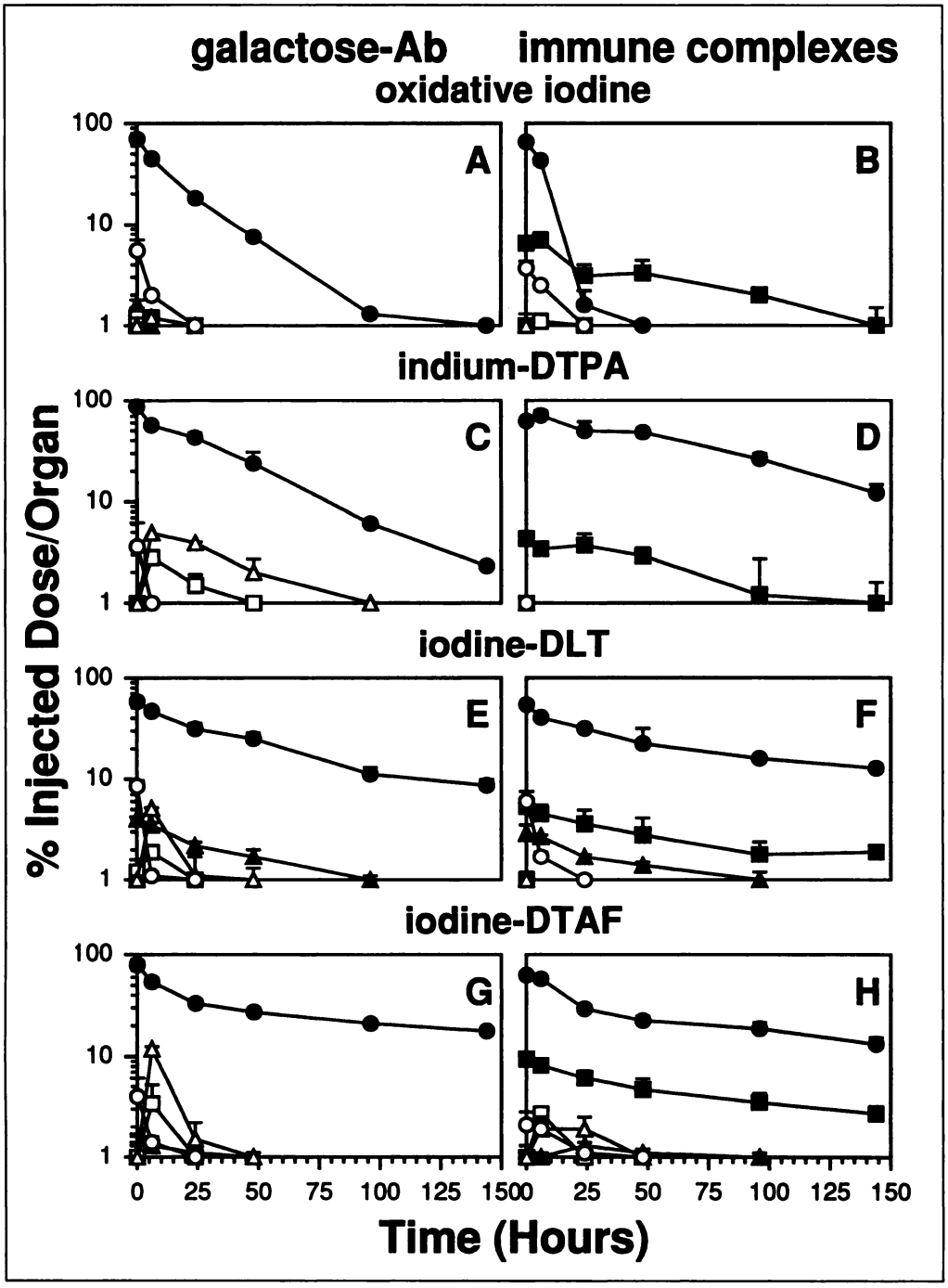

FIGURE 1. Biodistribution of radiolabeled Abs injected as either galactose conjugates (left panels) or immune complexes (right panels). The labels used were conventional iodine (oxidative), ^{111}In-DTPA, ^{125}I-DLT or ^{125}I-DTAF, as indicated. The tissues examined were the blood, liver, spleen, kidneys, small intestine and large intestine. The entire organs were collected and counted for radioactivity. The total cpm in blood was calculated on the basis that blood constitutes 7.4% of body weight. (●), liver; (○), blood; (■), spleen; (▲), kidneys; (△), small intestine; (□), large intestine. Means ± s.d. are shown for two experiments, each including three mice. Intra-experiment variation was less than interexperiment variation. Any s.d. not seen are too small to be visible above the symbols. Symbols not seen indicate that such organs contained <1.0% of the injected dose.

basic issue is whether one of these cell types is more efficient than the other in disposing of the cleared label. Second, considering that the hepatocyte is the only cell in the body that can deliver catabolic products to bile, we considered that Kupffer cells were likely to be more similar to tumor cells in their handling of lysosomally trapped material, although tumor cells may not be exactly the same as Kupffer cells in this regard.

Four radiolabels were tested after conjugation to IgG; namely, two residualizing labels (^{111}In-DTPA and ^{125}I-DLT), one label that has shown partial retention within cells (^{125}I-DTAF) (*21*) and a conventional oxidative iodine label, for comparison. These were injected in two forms, either galactosylated (for delivery to hepatocytes) or in immune complexes (for delivery to Kupffer cells and macrophages) in normal mice. The biodistribution at various time points was determined by sacrificing successive groups of mice, and the results are summarized in Figures 1–3. Although our primary interest was in the processing of radiolabels by the liver, we also examined the blood, spleen, kidney, small intestine and large intestine. The cpm present in these other organs were generally very low compared with the cpm in the liver, but some interesting patterns were apparent. The radioactivity in the blood was assayed in order to confirm rapid clearance from the blood. The first time point was selected to be the time at which liver cpm were at the peak, as determined in preliminary experiments: for galactosylated Abs, this was 5 min after injection; for immune complexes, 15 min after injection.

Blood clearance was significantly faster with the galactosylated Abs than with the immune complexes but was sufficiently fast with immune complexes for the purpose of these experiments. The spleen displayed considerable uptake of immune complexes, as expected, although much less than the liver.

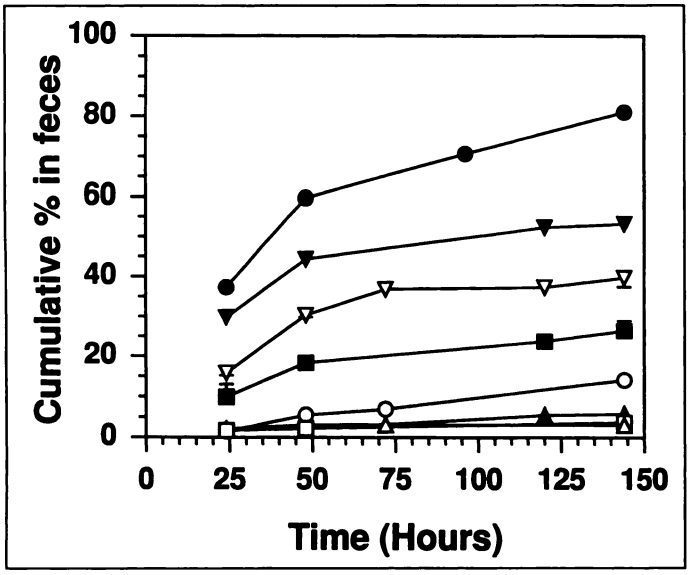

FIGURE 2. Cumulative fecal excretion of radiolabeled Abs injected as either galactose conjugates (closed symbols) or immune complexes (open symbols). Feces were collected in one of the experiments described in Figure 1 for each radiolabel. The radiolabels used were: triangles, conventional iodination; circles, indium-DTPA; squares, iodine-DLT; inverted triangles, iodine-DTAF.

However, cpm taken up by the spleen, in marked contrast to cpm taken up by the liver, were catabolized very slowly. Therefore, for the rapidly excreted radiolabel, conventional iodine, the spleen contained more cpm than the liver at 24 hr and later time points (Fig. 1B). The prolonged retention of immune complexes in the spleen in a noncatabolic compartment has been described (*7,22*). Residualizing labels were not retained much longer by the spleen than conventional iodine, indicating that the rate of excretion of catabolic products is not the limiting factor for spleen retention. Cpm in the intestines appeared to give a clear indication of biliary excretion, even though the level of cpm present in these organs at any one time was low. We note that the entire small and large intestine was collected, including the contents. The peak cpm level in the small intestine and in the large intestine was at 3 hr (Fig. 1C,E,G, H). With the residualizing labels indium-DTPA and iodine-DLT, significant cpm in the intestines were seen only with the galactose conjugates and not with immune complexes. In contrast, iodine-DTAF was detected in the intestines when injected in either form. These results were entirely consistent with results obtained from analysis of feces, collected in the same experiments, as described below. Significant kidney uptake was detected only for iodine-DLT and was essentially the same independent of the form in which the radiolabel was injected. These results also are consistent with other evidence that DLT is excreted by urine rather than bile (*23*).

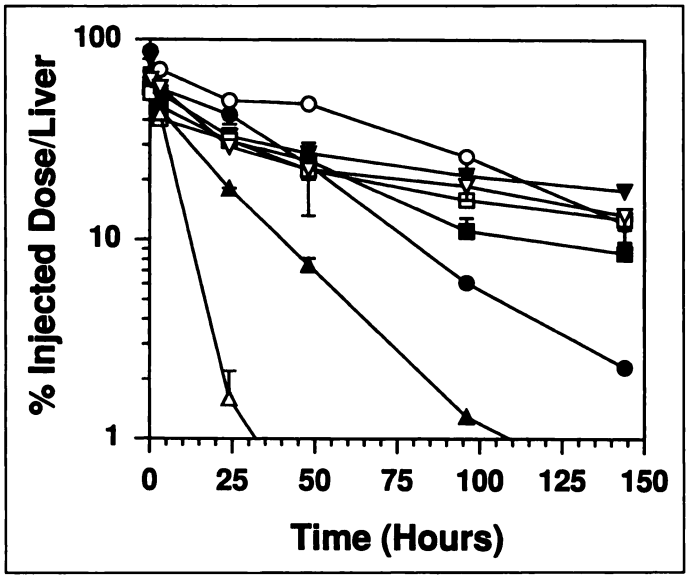

FIGURE 3. Liver catabolism of radiolabeled Abs injected as either galactose conjugates (closed symbols) or immune complexes (open symbols). These data are from the same experiments as Figure 1 but are compiled to display differences in liver processing. Symbols are described in the Figure 2 legend. Means ± s.d. are shown for two experiments, each including three mice. Intra-experiment variation was less than interexperiment variation. Any s.d. not seen are too small to be visible above the symbols.

Figure 2 displays data obtained by analysis of the feces collected in the same experiments. This figure demonstrates large differences in fecal cpm, an indication of biliary excretion. In particular, the two residualizing labels, indium-DTPA and iodine-DLT, show marked differences in biliary excretion, although in many previous in vitro and in vivo experiments these two labels have appeared to be identical (*11,24*). With indium-DTPA, by day 6, 81% of the cpm from galactose conjugates was excreted in bile, compared with only 14% after injection of immune complexes. In contrast, with the iodine-DLT label, only 26% of the galactose conjugate was excreted by bile. The conventional iodine label did not collect in bile with either form of injection, and the iodine DTAF label was excreted largely in bile regardless of the form injected. Thus, with iodine-DTAF immune complexes, 40% was excreted in feces in 6 days, which was only 13% less than the amount excreted by an iodine-DTAF-galactose-Ab conjugate. These results with DTAF therefore demonstrate that, for labels with an affinity for biliary excretion, delivery directly to hepatocytes is not required, and degradation products of proteins catabolized in Kupffer cells can be efficiently delivered to bile, after release from the Kupffer cell.

Figure 3 is a compilation of the liver data from the same experiments and displays more clearly the difference between radiolabels. One interesting point is that, with the conventional iodine label, immune complexes were catabolized and excreted much faster than galactose conjugates. The liver clearance half-life was only 4.4 hr (r coefficient 0.999) for the conventional ^{125}I-immune complexes and 17.4 hr (r coefficient 0.995) for the conventional ^{125}I-gal-Ab. This is the opposite of the "desired" results in these experiments but may be useful for some purposes. Our experiments do not distinguish between the rates of internalization and the rates of catabolism and release of degradation products; however, it is known that internalization by the ASGP receptor is very fast, so it seems most likely that differences in catabolic rate are responsible for the differences observed in the processing of the conventional iodine label. Our purpose was to identify labels that were catabolized more rapidly by hepatocytes than by Kupffer cells, and of the four labels tested, only indium-DTPA had this property. At day 6, the liver retention was only 2.3% of the injected dose of the galactose conjugate (liver clearance half-life 28.2 hr with r coefficient 0.995) and was 5.3-fold higher with immune complexes (liver clearance half-life 57.6 hr with r coefficient 0.986). In contrast, with iodine-DLT and iodine-DTAF, the form of Ab injected had little effect on liver retention. Furthermore, indium-DTPA was retained longer in Kupffer cells than any of the other radiolabels tested. Based on these results, indium-DTPA was selected for the tumor localization experiments described below.

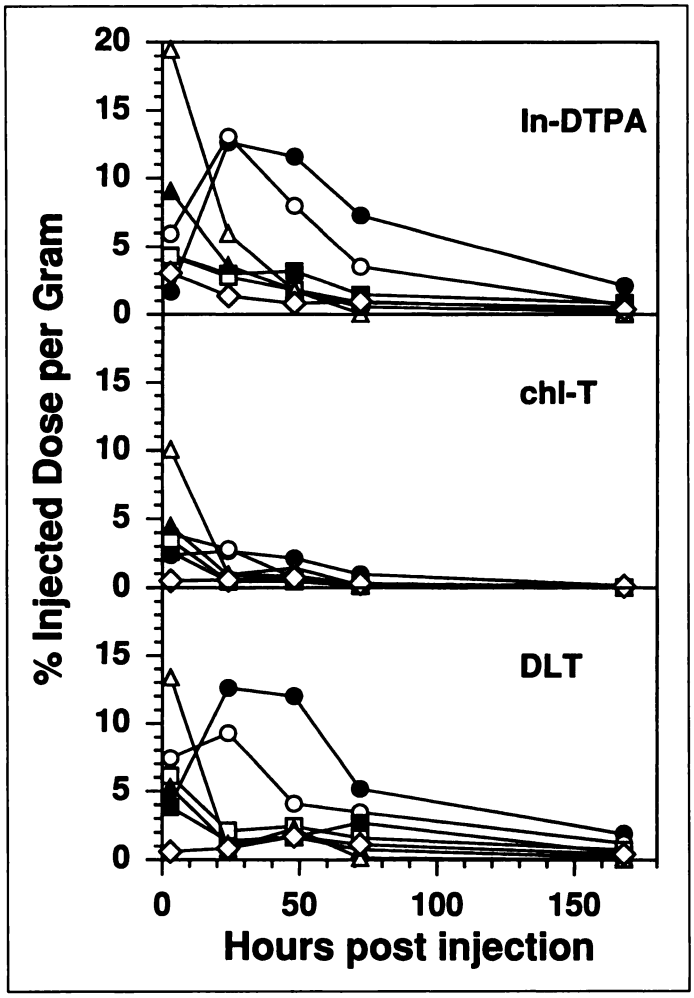

FIGURE 4. Biodistribution of radiolabeled gal-RS11 in nude mice bearing Calu-3 lung carcinoma xenografts subcutaneously. The %ID/g of tissue is shown. The Ab was labeled as indicated. "chl-T" indicates a conventional iodination with chloramine-T. The DLT and chl-T labels were tested in the same experiment using oxidative ^{125}I and ^{131}I-DLT. Mice were coinjected with asialo-BSM to temporarily block the ASGP receptor; in the indium-DTPA experiment, mice were given three injections of asialo-BSM, while four injections were given in the experiments with the other two labels, always at intervals of 8–12 hr. Tissues shown are: (●), Calu-3; (○), liver; (■), spleen; (□), kidney; (▲), lungs; (△), blood; (◇), muscle. Means of five animals per group are shown; s.d. are omitted for clarity.

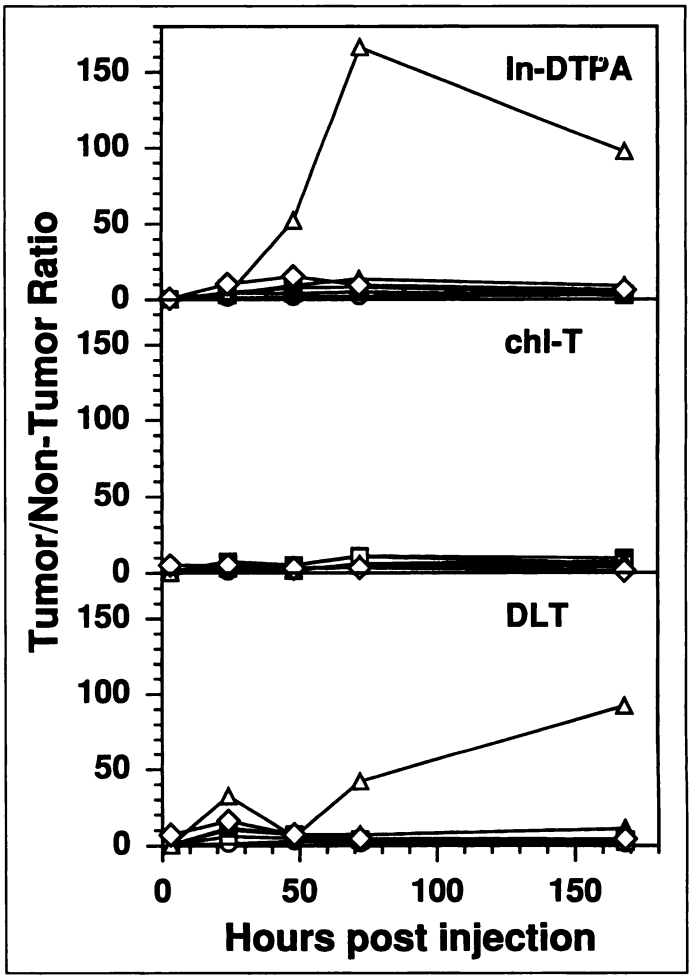

FIGURE 5. Biodistribution of radiolabeled gal-RS11 in nude mice bearing Calu-3 lung carcinoma xenografts subcutaneously. The tumor/nontumor ratios are shown. Other details are described in the Figure 4 legend. Because the tumor/blood ratios are so high, results for other tissues cannot be seen and are therefore shown in Figure 6 with a different scale on the y-axis.

Indium-111-DTPA as an Ab Label for Radioimmunodetection in Conjunction with Delayed Rapid Blood Clearance by Hepatocytes

The results described above demonstrate that indium-DTPA has the desired property of biliary excretion from hepatocytes and more rapid catabolism by hepatocytes than by Kupffer cells. Previous studies demonstrated that this label was retained well by the Calu-3 tumor in an in vivo nude mouse model system (*11*), using Ab RS11. Thus, this system seemed ideal to investigate the advantage of delayed rapid blood clearance by the ASGP receptor combined with a residualizing radiolabel. Tumor-bearing mice were injected with galactosylated ^{111}In-DTPA-RS11 and simultaneously with a large dose of asialo-BSM. Two additional injections of asialo-BSM were administered over the next 24 hr to effectively block the ASGP receptor. After the asialo-BSM was consumed, the galactosylated Ab was cleared efficiently from the blood. At various time points, groups of mice were killed, and the biodistribution of radiolabel determined. While our prediction was that indium-DTPA was the optimal label for this purpose, the same experiment was performed with a conventional iodine label and with iodine-DLT, for comparative purposes and to see if the differences predicted, based on the above data, would in fact occur. These experiments with the iodine labels included an additional, fourth, injection of asialo-BSM, to delay clearance for approximately an additional 12 hr. The slightly earlier clearance was considered to be an advantage for the ^{111}In-label due to its short half-life, 2.8 days, although this change had no detectable effect on the results. Results are shown in Figures 4–6, which display the %ID/g and the tumor/nontumor ratios.

Blood levels were generally as expected, with substantial blood levels for 2 days, followed by rapid clearance. At day 3, blood levels were <0.1% of the injected dose per gram of blood. However, it should be noted that the blood Ab concentration was considerably lower than that obtained with a nongalactosylated Ab. For example, in the previous study with DTPA-RS11, the mean blood levels were 11.6% at 1 day and 9.3% at 3 days, whereas in this study with DTPA-gal-RS11 the blood levels were 6.0% at 1 day and 1.7% at 2 days. This result indicates that hepatic uptake of the gal-Ab was not completely blocked by the asialo-BSM, which was also observed previously (*8*), and that is not unexpected, since the asialo-BSM is a competitive inhibitor for the ASGP receptor and cannot completely block uptake of gal-Abs.

The slight increase in the blood level from 24 to 48 hr with the DLT label and, to a lesser extent, with the chloramine T

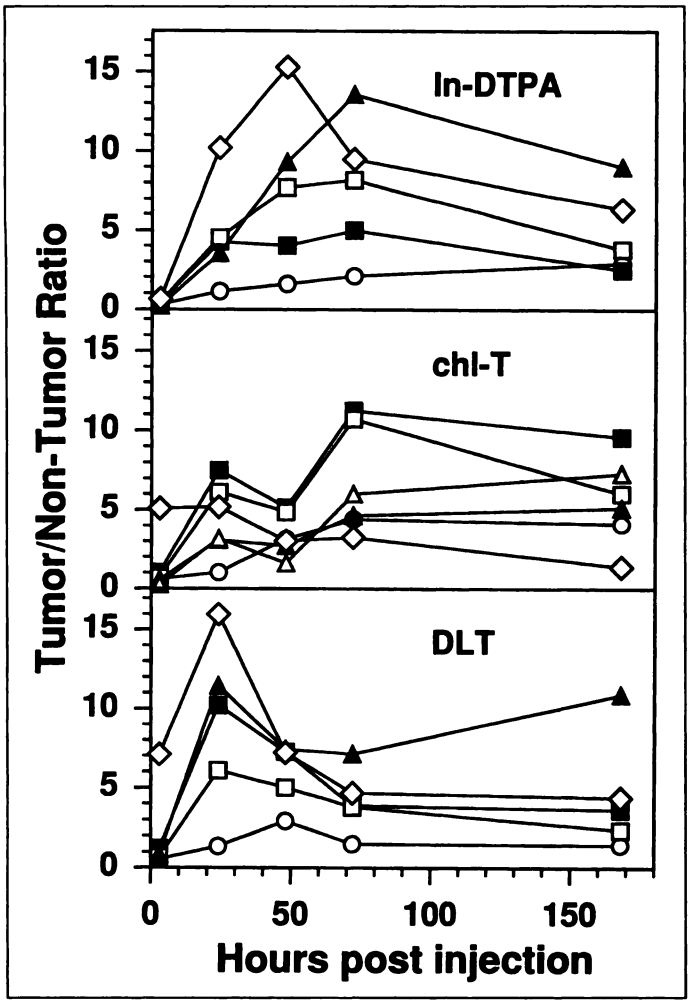

FIGURE 6. Biodistribution of radiolabeled gal-RS11 in nude mice bearing Calu-3 lung carcinoma xenografts subcutaneously. This is the same experiment as shown in Figure 5, with a different scale on the y-axis. The data for blood are shown only for the conventional iodine label, since the blood ratios obtained with the other two labels are off-scale. Although tumor/nontumor ratios are relatively high with the conventional chl-T iodine label, especially for the spleen and kidney, it should be noted that the absolute uptake in the tumor of this label is much less than with the two residualizing labels, as shown in Figure 4.

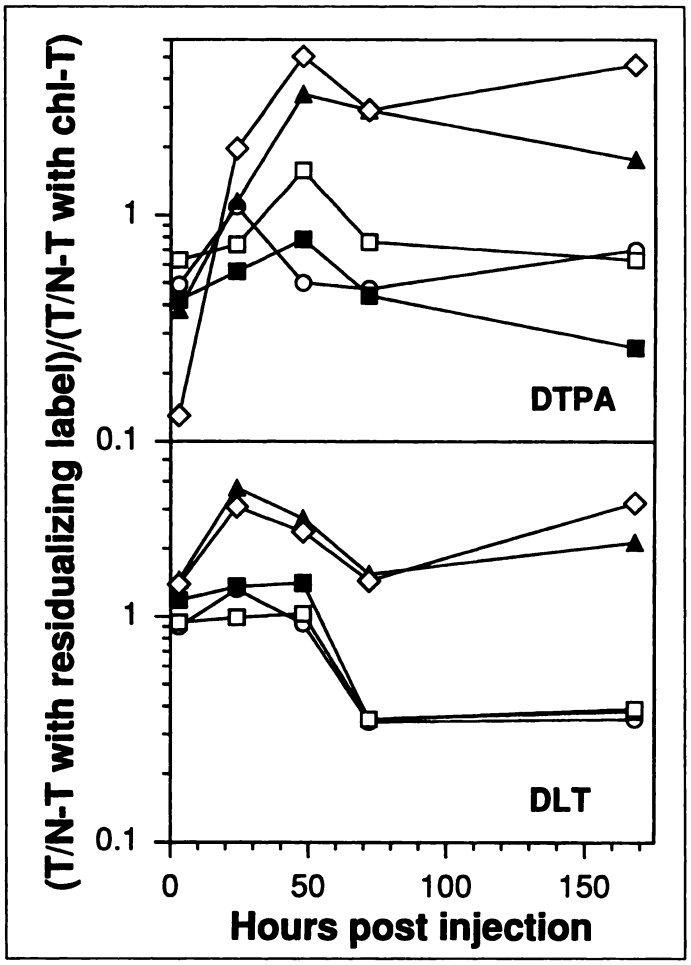

FIGURE 7. Comparison of residualizing labels indium-DTPA or iodine-DLT with a conventional iodine label. The y-axis shows the ratio (tumor/nontumor ratio with a residualizing label)/(tumor/nontumor ratio with a chloramine-T label). The experiments are the same as described in Figures 4–6, and the symbols are as shown in the Figure 4 legend. The blood is not included because the values would be off-scale but are described in the text.

label, would not be expected, and can be attributed to an experimental artifact. The explanation is that the 24-hr mice were collected without injection of the third dose of asialo-BSM, since they were to be killed at the same time as this injection, but they were inadvertently killed 1–2 hr late. In these mice, the inhibitor asialo-BSM from the two earlier injections was just depleted at this time, and thus significant Ab was cleared from the blood during this 1–2 hr interval. Accordingly, the true blood level at 24 hr is somewhat greater than that shown in Figure 4. This factor explains the small peak in the DLT blood curve at 24 hr in Figure 5 (top), and also probably contributes to the 24-hr peak in the DLT curves in Figure 6 (bottom), but does not substantially affect the overall shape of the curves, and only the 24-hr time point is affected.

Figures 4 and 5 show that the use of residualizing labels, both indium-DTPA and iodine-DLT, provides a large advantage in this tumor/Ab system, as shown previously in experiments with a simple injection of nongalactosylated Ab (*11*). The absolute amount of Ab in the tumor was lower than in the previous experiments due to the fact that the blood level of the Ab was not as high over the first 2 days, as noted above. Very high tumor/blood ratios were obtained, 166:1 with indium DTPA at 72 hr and 92:1 with DLT at 168 hr. However, such high tumor/normal tissue ratios were not obtained for the other organs tested, the liver, spleen, kidney, lungs and muscle. Due to the very high ratios obtained for the blood, the results with other tissues cannot be clearly seen in Figure 5. Therefore, Figure 6 shows results for tissues other than the blood. To show more clearly the effect of the residualizing label, Figure 7 is a plot of the ratio, (tumor/nontumor ratio with a residualizing label)/(tumor/nontumor ratio with a conventional iodine label). This graph clearly shows the distinction between the tissues that gain from use of a residualizing label, the lungs and muscle, and those which do not gain, the liver, spleen and kidneys. However, even for the lungs and muscle, the advantage of the residualizing labels is much less than for the blood. For the blood, this ratio would reach 33:1 for DTPA and 13:1 for DLT.

A basic question is whether the various radiolabels are cleared from normal tissue as efficiently as from blood. If not, this implies that the labels were retained, in some form, within the tissues. Several mechanisms of retention are possible, but if residualizing labels are retained more than nonresidualizing labels, this would strongly suggest that the labeled Abs were internalized and catabolized by the cells. Figure 5 strongly suggests that clearance of the residualizing labels from normal tissues is much less efficient than from the blood, but Table 1 summarizes the data that are directly relevant to this question, from the same experiment. This table shows the ratio of the (%

TABLE 1
Comparison of gal-Ab Clearance from Tissues and Blood

Label	Time	Tissue/blood ratio of % injected dose/g					
		Calu-3	Liver	Spleen	Kidney	Lungs	Muscle
^{125}I	Day 2	1.50	0.50	0.31	0.34	0.59	0.49
	Day 3	5.59	1.29	0.65	0.71	1.24	1.76
DLT	Day 2	5.28	1.80	0.74	1.07	0.73	0.75
	Day 3	39.77	26.62	20.69	12.31	5.69	8.69
DTPA	Day 2	6.64	4.58	1.83	1.03	1.03	0.47
	Day 3	145.40	70.40	29.20	17.60	10.80	18.80

In these experiments, the Ab was cleared rapidly from the blood on days 2–3, so by day 3 the blood level was <0.1% injected dose/g. The radiolabels used were conventional ^{125}I, ^{125}I-DLT and ^{111}In-DTPA.

injected dose/g of tissue)/(% injected dose/g of blood) at days 2 and 3, the time during which efficient blood clearance occurred. As shown, this ratio increased greatly over this time period for all normal tissues with residualizing labels, while the increase was much less with a conventional iodine label. This is not surprising for the liver and kidney, since these are directly involved in the catabolism occurring, but note that a similar effect occurred for the lungs and muscle. We conclude, therefore, that some of the label appears to be internalized and catabolized by cells in all normal tissues tested.

Since one of the expected advantages of the indium-DTPA label, as explained in the first part of this paper, is due to its biliary excretion, it is interesting to examine the tumor/liver ratio with indium-DTPA in comparison with iodine-DLT, which is not excreted in bile. As shown in Figure 6, the tumor/liver ratio with indium-DTPA increased from 72 hr to 168 hr, whereas tumor/normal tissue ratios decreased for all other organs tested. Furthermore, this increase in the tumor/liver ratio did not occur with the DLT label, as predicted. This improvement in the tumor/liver ratio with indium-DTPA, but not with DLT, is also displayed in Figure 7. However, the magnitude of this effect is small compared with the other processes occurring.

Dosimetry calculations were performed to evaluate the method described in comparison with simple injection of nongalactosylated ^{111}In-DTPA-RS11, which was previously tested (*11*). When normalized to a 1,500 cGy dose to blood, the tumor dose, in the experiment described above, would be 2,880 cGy, or 1.9 × the blood dose, with a ^{90}Y label, assuming that the biodistribution of yttrium and indium is the same. In comparison, using a simple injection of ^{88}Y-DTPA-RS11, the tumor radiation dose was calculated to be 2.9 × the blood dose. A major difference between the two experiments is the total injected dose localizing to the tumor, which peaked at 12.6% injected dose/g here but reached 43.2% in the earlier experiments. This difference can be attributed to the lower level of circulating Ab in the experiments described here and clearly constitutes a disadvantage of this approach.

DISCUSSION

The experiments reported here were designed to investigate some of the possible manipulations that can be performed to optimize radioimmunotherapy (RAIT). Very high tumor/blood ratios were obtained, 166:1 at 72 hr, which is >10-fold higher than the highest tumor/blood ratio observed in previous experiments using a simple Ab injection. Therefore, this approach may be useful for certain purposes. However, the studies described here have not resulted in an improved therapeutic ratio, at least as judged by dosimetry calculations. The reason that these high tumor/blood ratios do not translate into an improved therapeutic ratio is because blood clearance is much faster with the new method, so a much smaller fraction of the injected dose reaches the tumor at all time points. Clearly, the high tumor/nontumor ratios are due to the fact that blood levels are very low. In any type of Ab therapy, the initial tumor/blood localization ratios are low, since it takes some time for the Ab to exit the vascular space and reach the antigens on the tumor cells. This represents an unavoidable starting disadvantage, which must be overcome by the later accumulation of Ab in the tumor, coupled with clearance from the blood. It is useful to more specifically compare these results with previous data obtained with directly labeled Ab (*11*), in the same experimental system, with DTPA-RS11. At the 24 hr time point, the mean tumor/blood ratios were similar (2.7 versus 2.5). However, the mean % injected dose/g (%ID/g) was reduced 2.2-fold (12.6% versus 28.2%). At day 3, although the mean tumor/blood ratio was dramatically increased (166.4 versus 4.4), the %ID/g in tumor was reduced fivefold (7.3% versus 40.5%). The dosimetry calculations indicated that the high tumor/blood ratios at later time points did not overcome the disadvantage of these relatively low values of tumor Ab accretion.

We would emphasize three major conclusions from these data. First, the data demonstrate a marked difference between the two residualizing labels ^{111}In-DTPA and ^{125}I-DLT. This is important, because in all previous studies, in vitro and in vivo, these labels appeared to be processed identically. The difference is in biliary excretion from hepatocytes, which is the major route of excretion for indium-DTPA delivered to hepatocytes. Similar differences between residualizing labels have been described, although the labels used by other investigators were different. For example, Strobel et al. described differences between two forms of DLT, differing in the method of conjugation to protein: cyanuric chloride conjugates showed more biliary excretion than conjugates prepared by reductive amination (*23*). Arano et al. described differences between protein conjugates of isothiocyanato-benzyl-ethylenediaminetetraacetate (EDTA) and the cyclic anhydride of DTPA (*16*) and also differences between two types of benzyl-EDTA conjugates (*17*). Their studies also investigated differences between hepatocytes and Kupffer cells, although using a different delivery method for Kupffer cells, the mannose receptor. Their data suggest that benzyl-EDTA may be an excellent label for the approach described here, since it was very rapidly excreted from hepatocytes, whereas it was retained much longer by Kupffer cells. It has not yet been determined whether benzyl-EDTA is retained within tumor cells in vitro as well as benzyl-DTPA (although this seems likely).

The study by Arano et al. provides many interesting comparisons with our data (*16*). The DTPA conjugate used by these

investigators, unlike our DTPA conjugates, showed similar retention in both hepatocytes and Kupffer cells; this may be due to the different conjugates used, with Arano et al. using direct conjugation of the cyclic anhydride, compared with our use of the isothiocyanato-benzyl-DTPA conjugate. Indeed, the results of Arano et al. with benzyl-EDTA are quite similar to our results with benzyl-DTPA, in that excretion from hepatocytes was much faster than excretion from Kupffer cells. An apparent difference is that the excretion of the benzyl-EDTA conjugates seemed much faster than the excretion of benzyl-DTPA conjugates described here. However, we would suggest that most or all of this difference may be attributed to the different proteins used in the conjugates: albumin compared with IgG_{2a}. From results with conventional iodine labels, it is clear that different proteins are catabolized by hepatocytes at different rates, and IgG is catabolized relatively slowly. For example, in our previous experiments, hepatocyte catabolism of asialo-fetuin was very rapid, with >95% excretion from the liver within 1 hr. In contrast, with conventional ^{125}I-IgG, 45% of the cpm were still present in the liver at 3 hr, as shown here. Although speculative, these data suggest that the catabolic rate of various proteins within lysosomes also can have a significant impact on the excretion rate from the liver. We conclude that benzyl-DTPA and benzyl-EDTA are similar in their processing behavior, and proof of any differences between them will require direct comparisons.

The difference between hepatocyte excretion of DTPA and DLT suggests that there is an important aspect of the metabolism of these residualizing labels that is not currently understood. That is, if delivery of DTPA from lysosomes to bile occurs by exocytosis (*12,13*), and if DLT is trapped within lysosomes together with DTPA, than DLT should also be excreted in bile. Further experiments are required to explain this apparent anomaly. The possible explanations are: (a) DLT is excreted into bile, but is rapidly reabsorbed, so that it is never detected in the bile or the intestines (as is DTPA); (b) DLT is trapped primarily in the cytoplasm rather than within lysosomes, but if this were true, it would be expected that retention of DLT within cells would be less efficient than retention of DTPA, which does not appear to be the case (*24*) (but see below); or (c) both DTPA and DLT are primarily trapped within the cytoplasm, rather than in lysosomes, and DTPA is selectively transported into bile.

Another, less dramatic difference between DTPA and DLT was also observed in their retention by Kupffer cells after delivery as immune complexes: DTPA was retained significantly longer than DLT (Fig. 3). As noted above, the retention of these two radiolabels has previously been identical, in a variety of tumor cell lines in vitro and in Calu-3 lung carcinoma cells in vivo. Possibly, the relative handling of the two labels is dependent on the particular cell type, but further experiments are required to investigate this possibility.

The second major conclusion is that radiolabels may be processed very differently by hepatocytes and Kupffer cells and, therefore, the effect of delayed rapid blood clearance will be dependent on the mechanism of rapid clearance used. This difference is shown clearly by the DTPA results and was demonstrated previously by Arano et al. with different radiolabels (*16*).

The third conclusion is that two-phase blood clearance by the ASGP receptor produces very high tumor/blood ratios (since clearance from blood is very efficient) but does not produce equally high tumor/normal tissue ratios for other organs when residualizing labels are used. The data suggest that the radiolabels are retained intracellularly. This is as expected for the liver, spleen and kidney, but why should the muscle and lungs internalize circulating Ab? Because this was not seen with nongalactosylated Ab (*11*), it appears that uptake by lungs and muscle is due to recognition of galactose. Although this possibility is speculative at this time, it is consistent with the fact that galactose-binding lectins are present in many animal tissues (*25–27*). Since the inhibitor we use to block the ASGP receptor, asialo-BSM (the most avid ligand known for the ASGP receptor), contains galactosamine rather than galactose, it is possible that it does not efficiently block all galactose-binding receptors.

Having realized that, with the approach used here, residualizing labels accumulate in all normal cells, including muscle and lung, we can begin to develop methods of circumventing this problem. Since a large fraction of bound Ab remains on the surface of tumor cells (*28*), but is likely to be rapidly internalized by other cells (*29*), it may be possible to exploit this difference. For example, there is currently much interest in pretargeting strategies, in which a small radiolabeled molecule (such as ^{111}In-DTPA-biotin) is injected after an appropriate Ab conjugate (such as Ab-streptavidin) is bound to the tumor and cleared from the blood. In this approach the labeled ligand will bind only to the Ab present on the cell surface but not to internalized Ab. Thus, this approach would fit well with the strategy described here, and experiments in this direction are in progress.

A difficulty encountered in these experiments is that the galactosylated Abs were always cleared much more rapidly than control Abs. For this reason, the absolute tumor uptake of the gal-Abs was always much less than the maximum uptake of a control Ab. As noted above, there are two possible explanations for this: (a) inhibition of the ASGP receptor is not complete and (b) gal-Abs are taken up by other galactose-binding receptors. Development of more efficient methods of inhibiting the ASGP receptor are possible, for example, by using antibodies to the ASGP receptor that might function as irreversible inhibitors. Another approach is to combine the two major strategies of delayed rapid blood clearance, as described in the Introduction, by using a galactosylated cross-linking reagent, an approach developed by Bagshaw and collaborators (*30*). Although cross linking normally sends the complexes to Kupffer cells, it seems likely that a galactosylated cross-linking agent would tend to deliver the complexes to hepatocytes. This was demonstrated by Marshall et al. (*7*), using galactosylated streptavidin as a clearing agent for biotinylated Abs; complexes produced by control streptavidin, in contrast, were deposited in Kupffer cells. When complexes are formed with a galactosylated second Ab, these will be recognized by macrophages/Kupffer cells by Fc receptors but will also be recognized by the ASGP receptor on hepatocytes. Which of these receptors will dominate is difficult to predict, and may depend on the exact conditions, but can be investigated by using some of the results described here. For example, with an indium-DTPA label, excretion by bile would indicate uptake by hepatocytes, whereas excretion by urine would indicate uptake by Kupffer cells.

It would seem feasible to perform similar experiments in humans, although clearly large amounts of asialo-BSM, or other suitable inhibitor, would be required. The possibility of toxicity resulting from this approach was previously discussed (*8*); we have not observed evidence of toxicity in mice (*8*), and there is no reason to suspect that toxicity would be greater in man. Considering that bovine and ovine submaxillary glands are the source of the best-known inhibitors, there would seem to be an abundant supply. The experiments described here should be

considered initial investigations on ways of manipulating blood clearance and catabolism of the radiolabel. Further studies in this direction will, we believe, lead to the desired goal of maximizing tumor uptake, while minimizing uptake by normal tissues.

CONCLUSION

While various residualizing radiolabels are retained similarly within tumor cells, they can differ markedly in the extent to which they are excreted by hepatocytes into bile. We used a radiolabel, ^{111}In-benzyl-DTPA, which is rapidly excreted by hepatocytes, as an Ab label, in conjunction with a delayed rapid blood clearance method that delivers the Ab efficiently to hepatocytes. The very high tumor/blood localization ratios obtained were not matched by other high tumor/normal tissue ratios, but the results are encouraging for further development of this approach.

ACKNOWLEDGMENTS

We are grateful to Dr. Gary Griffiths, Philip Andrews and Don Varga for assistance with radiolabeling; to Susan Chen for cell culture; and to Rosarito Aninpot for assistance with mouse experiments. This work was supported in part by National Institutes of Health grants CA63624, CA 60039 and CA39841.

REFERENCES

1. Jurcic JG, Scheinberg DA. Radioimmunotherapy of hematological cancer: problems and progress. *Clin Cancer Res* 1995;1:1439–1446.
2. Ong GL, Mattes MJ. Penetration and binding of antibodies in experimental human solid tumors grown in mice. *Cancer Res* 1989;49:4264–4273.
3. Fenwick JR, Philpott GW, Connett JM. Biodistribution and histological localization of anti-human colon cancer monoclonal antibody (MAb) 1A3: the influence of administered MAb dose on tumor uptake. *Int J Cancer* 1989;44:1017–1027.
4. Sharkey RM, Boerman OC, Natale A, et al. Enhanced clearance of radiolabeled murine monoclonal antibody by a syngeneic anti-idiotype antibody in tumor-bearing nude mice. *Int J Cancer* 1992;51:266–273.
5. Pedley RB, Dale R, Boden JA, Begent RHJ, Keep PA, Green AJ. The effect of second antibody clearance on the distribution and dosimetry of radiolabeled anti-carcinoembryonic antigen antibody in a human colonic tumor xenograft model. *Int J Cancer* 1989;43:713–718.
6. Paganelli G, Magnani P, Zito F, et al. Three-step monoclonal antibody tumor targeting in carcinoembryonic antigen-positive patients. *Cancer Res* 1991;51:5960–5966.
7. Marshall D, Pedley RB, Melton RG, Boden JA, Boden R, Begent RHJ. Galactosylated streptavidin for improved clearance of biotinylated intact and $F(ab')_2$ fragments of an anti-tumor antibody. *Br J Cancer* 1995;71:18–24.
8. Ong GL, Ettenson D, Sharkey RM, et al. Galactose-conjugated antibodies in cancer therapy: properties and principles of action. *Cancer Res* 1991;51:1619–1626.
9. Norrgren K, Strand S-E, Nilsson R, Lindgren L, Sjögren H-O. A general, extracorporeal immunoadsorption method to increase the tumor-to-normal tissue ratio in radioimmunoimaging and radioimmunotherapy. *J Nucl Med* 1993;34:448–454.
10. Thorpe SR, Baynes JW, Chroneos ZC. The design and application of residualizing labels for studies of protein catabolism. *FASEB J* 1993;7:399–405.
11. Stein R, Goldenberg DM, Thorpe SR, Basu A, Mattes MJ. Effects of radiolabeling monoclonal antibodies with a residualizing iodine radiolabel on the accretion of radioisotope in tumors. *Cancer Res* 1995;55:3132–3139.
12. Renaud G, Hamilton RL, Havel RJ. Hepatic metabolism of colloidal gold-low-density lipoprotein complexes in the rat: evidence for bulk excretion of lysosomal contents into bile. *Hepatology* 1989;9:380–392.
13. Kornfeld S, Mellman I. The biogenesis of lysosomes. *Annu Rev Cell Biol* 1989;5:483–525.
14. Bockow B, Mannik M. Clearance and tissue uptake of immune complexes in complement-depleted and control mice. *Immunology* 1981;42:497–504.
15. Skogh T, Blomhoff R, Eskild W, Berg T. Hepatic uptake of circulating immunoglobulin G immune complexes. *Immunology* 1985;55:585–594.
16. Arano Y, Mukai T, Uezono T, et al. A biological method to evaluate bifunctional chelating agents to label antibodies with metallic radionuclides. *J Nucl Med* 1994;35:890–898.
17. Arano Y, Mukai T, Akizawa H, et al. Radiolabeled metabolites of proteins play a critical role in radioactivity elimination from the liver. *Nucl Med Biol* 1995;22:555–564.
18. De Leij L, Helrich W, Stein R, Mattes MJ. Small cell lung cancer–cluster-2 antibodies detect the pancarcinoma/epithelial glycoprotein EGP-2. *Int J Cancer* 1994;8(suppl):60–63.
19. Leung SO, Goldenberg DM, Dion AS, et al. Construction and characterization of a humanized, internalizing B-cell (CD22)-specific, leukemia/lymphoma antibody, LL2. *Mol Immunol* 1995;32:1413–1427.
20. Leung SO, Shevitz J, Pellegrini MC, et al. Chimerization of LL2, a rapidly internalizing antibody specific for B-cell lymphoma. *Hybridoma* 1994;13:469–476.
21. Harapanhalli RS, Schafranek W, Ong GL, Mattes MJ. Lysine-directed radioiodination of proteins with a cyanuric chloride derivative of aminofluorescein. *Anal Biochem* 1995;231:50–56.
22. Goldenberg DM, Sharkey RM, Ford E. Anti-antibody enhancement of iodine-131 anti-carcinoembryonic antigen radioimmunodetection in experimental and clinical studies. *J Nucl Med* 1987;28:1604–1610.
23. Strobel JL, Baynes JW, Thorpe SR. Iodine-125-glycoconjugate labels for identifying sites of protein catabolism in vivo: effect of structure and chemistry of coupling to protein on label entrapment in cells after protein degradation. *Arch Biochem Biophys* 1985;240:635–645.
24. Shih LB, Thorpe SR, Griffiths GL, et al. The processing and fate of antibodies and their radiolabels bound to the surface of tumor cells in vitro: a comparison of nine radiolabels. *J Nucl Med* 1994;35:899–908.
25. Kempka G, Roos PH, Kolb-Bachofen V. A membrane-associated form of C-reactive protein is the galactose-specific particle receptor on rat liver macrophages. *J Immunol* 1990;144:1004–1009.
26. Abdullah M, Kierszenbaum AL. Identification of rat testis galactosyl receptor using antibodies to liver asialoglycoprotein receptor: purification and localization on surfaces of spermatogenic cells and sperm. *J Cell Biol* 1989;108:367–375.
27. Monsigny M, Roche AC, Midous P, Kieda C, Mayer R. Endogenous lectins of myeloid and tumor cells: characterization and biological implications. In: Gabius HJ, Nagel GA, eds. *Lectins and glycoconjugates in oncology*. New York: Springer-Verlag; 1988:25–47.
28. Kyriakos RJ, Shih LB, Ong GL, Patel K, Goldenberg DM, Mattes MJ. The fate of antibodies bound to the surface of tumor cells in vitro. *Cancer Res* 1991;52:835–842.
29. van Deurs B, Peterson DW, Olsnes S, Sandvig K. The ways of endocytosis. *Int Rev Cytol* 1989;117:131–178.
30. Bagshaw KD. Towards generating cytotoxic agents at cancer sites. *Br J Cancer* 1989;60:275–281.